

Article

The First Deep-Sea Stylasterid (Hydrozoa, Stylasteridae) of the Red Sea

Davide Maggioni ^{1,2,*}, Tullia I. Terraneo ³, Giovanni Chimienti ^{4,5}, Fabio Marchese ³, Daniela Pica ^{5,6}, Stephen D. Cairns ⁷, Ameer A. Eweida ⁸, Mattie Rodrigue ⁹, Sam J. Purkis ¹⁰ and Francesca Benzoni ³

- ¹ Department of Earth and Environmental Sciences (DISAT), University of Milano-Bicocca, 20126 Milano, Italy
- ² Marine Research and High Education (MaRHE) Center, University of Milano-Bicocca, Faafu Magoodhoo Island 12030, Maldives
- ³ Red Sea Research Center, Division of Biological and Environmental Science and Engineering, King Abdullah University of Science and Technology (KAUST), Thuwal 23955, Saudi Arabia; tulliaisotta.terraneo@kaust.edu.sa (T.I.T.); fabio.marchese@kaust.edu.sa (F.M.); francesca.benzoni@kaust.edu.sa (F.B.)
- ⁴ Department of Biology, University of Bari Aldo Moro, 70125 Bari, Italy; giovanni.chimienti@uniba.it
- ⁵ Consorzio Nazionale Interuniversitario per le Scienze del Mare (CoNISMa), 00196 Rome, Italy; daniela.pica@szn.it
- ⁶ Department of Integrative Marine Ecology, Stazione Zoologica Anton Dohrn, 87071 Amendolara, Italy
- ⁷ Department of Invertebrate Zoology, National Museum of Natural History, Smithsonian Institution, Washington, DC 20013, USA; cairns@si.edu
- ⁸ Marine Conservation Program, Neom, Saudi Arabia; ameer.eweida@neom.com
- ⁹ OceanX, 37 West 39th St., New York, NY 10018, USA; mattie@oceanx.org
- ¹⁰ Department of Marine Geosciences, Rosenstiel School of Marine and Atmospheric Science, University of Miami, Miami, FL 33149, USA; spurkis@rsmas.miami.edu
- * Correspondence: davide.maggioni@unimib.it



Citation: Maggioni, D.; Terraneo, T.I.; Chimienti, G.; Marchese, F.; Pica, D.; Cairns, S.D.; Eweida, A.A.; Rodrigue, M.; Purkis, S.J.; Benzoni, F. The First Deep-Sea Stylasterid (Hydrozoa, Stylasteridae) of the Red Sea. *Diversity* **2022**, *14*, 241. <https://doi.org/10.3390/d14040241>

Academic Editor: Luc Legal

Received: 25 February 2022

Accepted: 22 March 2022

Published: 25 March 2022

Publisher's Note: MDPI stays neutral with regard to jurisdictional claims in published maps and institutional affiliations.



Copyright: © 2022 by the authors. Licensee MDPI, Basel, Switzerland. This article is an open access article distributed under the terms and conditions of the Creative Commons Attribution (CC BY) license (<https://creativecommons.org/licenses/by/4.0/>).

Abstract: The Stylasteridae, commonly known as lace corals, is a family of colonial calcifying hydrozoans mostly inhabiting deep waters. Stylasterids show a cosmopolitan distribution but, in some areas, they are characterized by low species diversity, such as in the Red Sea, where only a shallow-water species has been reported so far. With this work, we provide the first evidence of a deep-sea stylasterid inhabiting the NEOM region in the northern Saudi Arabian Red Sea, at depths ranging between 166 and 492 m. Morphological examinations revealed that this species was previously unknown and belonging to the genus *Stylaster*. We, therefore, describe *Stylaster tritoni* sp. nov., representing the first record of the genus in the Red Sea. Lastly, the phylogenetic position of the species within the Stylasteridae was evaluated, revealing a close relationship with shallow-water Indo-Pacific and Western Atlantic *Stylaster* species and confirming the polyphyletic nature of the genus *Stylaster*.

Keywords: *Stylaster*; *Stylaster tritoni*; lace coral; new species; new record; phylogeny

1. Introduction

Despite once being considered a homogeneous and abiotic environment, in the last decades, the deep sea has revealed an extraordinary diversity of life, habitats, and ecosystems [1,2]. The fast-paced technological progress in deep-sea research is constantly widening our knowledge on the diversity, ecology, and evolution of benthic deep-sea life [3]. Key advances, such as the development of manned and unmanned underwater vehicles, are allowing scientists to directly observe and sample deep-sea organisms in their natural environment, facilitating, for instance, biodiversity, distributional, and behavioral studies, as well as new species discovery (e.g., [4–7]).

Despite the flourishing deep-sea research, some areas remain poorly explored, such as the Red Sea basin. The Red Sea is a young and elongated body of water that stretches over 15° of latitude [8]. As a consequence, it is characterized by diverse environmental conditions

along its latitudinal gradient [9]. Overall, the Red Sea is characterized by environmental conditions which have been defined extreme, especially due to the high water temperature and salinity, and the strong seasonal fluctuations of several environmental variables. In its more surficial portion, the Red Sea seawater increases in temperature from north to south, while salinity follows an opposite trend, due to a higher evaporation rate, lack of freshwater input, and exchange with adjacent basins in the north [10]. In its deeper layers, the Red Sea water remains unusually warm and very saline compared to any other ocean, with water temperature never dropping below 21 °C and salinity around 40.5 PSU, thus providing unique environmental conditions and physiological challenges for the organisms which have adapted to live there [11,12].

In recent years, the shallow-water reef communities in the Red Sea have been increasingly investigated, even though many relevant topics may still be underrepresented compared to other better-studied coral reef systems [13–16]. The current knowledge on the shallow Red Sea marine life reveals this basin as a hotspot for biodiversity and endemism [17,18], mostly due to the peculiar geological history of this sea and the presence of multiple potential isolating barriers [10,19]. Regarding the deep-sea benthos, only a few studies have been conducted in the Red Sea compared to other areas (see Joydas et al. [20] and references therein), and information on some taxa, such as hydrozoans, is scant in literature.

Overall, Red Sea hydrozoans have been scarcely studied in the past, summing up to about 160 species [21,22], even though new species, new records, and possibly endemic cryptic genetic lineages have been recently identified thanks to an integrative taxonomic approach [23–26]. Indeed, this approach, which relies on combining multiple lines of evidence (such as morphology, genetics, and ecology) to delineate taxonomic units [27], is greatly improving our knowledge of the diversity and biogeography of different marine organisms globally and in the Red Sea (e.g., [28–30]). Hydrozoans play important ecological roles in shallow Red Sea waters, especially the calcifying hermatypic species [31,32], such as the three fire coral species of the area [33], which can become dominant in specific reef zones [31]. Another calcifying shallow-water species reported from the Red Sea is *Distichopora violacea* (Pallas, 1766), which is also the only member of the family Stylasteridae (Gray, 1847) recorded from the area so far [34].

Stylasterids, commonly known as lace corals, are colonial hydrozoans able to produce a calcium carbonate skeleton, similar to fire corals and scleractinians. They are generally smaller in size compared to Scleractinia and do not contribute much to shallow coral reef formation [35]. Only a few species are known to inhabit shallow waters, and Lindner et al. [36] demonstrated that this group originated and largely diversified in the deep sea and only later invaded shallower environments, at least four times. Most species (about 90%) inhabit waters deeper than 50 m [35,37] where, in some cases, they reach large size and densities, representing dominant and habitat-forming species in deep-water coral mounds [1]. A recent example is provided by Hoarau et al. [38], who described mesophotic (75–100 m deep) aggregations of the stylasterid *Stylaster flabelliformis* (Lamarck, 1816) and the scleractinians *Leptoseris* spp. in the Western Indian Ocean, providing a habitat for a diverse associated community of vertebrates and invertebrates.

Stylasterids are distributed almost ubiquitously [35], with a predominantly insular distribution [39] and with the tropical southwest Pacific region being the richest in terms of species [40]. However, several areas appear not to be suitable environments for lace corals, including large islands and continental masses [39]. Accordingly, only the widely distributed shallow-water *D. violacea* has been reported from the Red Sea [34], whereas no deep-sea stylasterid species had been found so far.

In this work, we present the first record of a deep-sea stylasterid and of the genus *Stylaster* (Gray, 1831) in the Red Sea, describing a new species and assessing its phylogenetic position within the family Stylasteridae.

2. Materials and Methods

From September to November 2020, shallow, mesophotic, and deep-sea explorations were carried out in the NEOM (the largest of the Saudi Arabia development giga-projects) area, on the Saudi Arabian coast of the Gulf of Aqaba and northern Red Sea, in the context of the OceanX-NEOM ‘Deep Blue’ Expedition aboard the M/V *OceanXplorer*. Sampling took place from two Triton 3300/3 submersibles (Nadir and Neptune) equipped with a Sonardyne Ranger Pro 2 system, light and camera systems including a Wide-Angle Red DSMC2 Helium 8K Canon CN-E15.5–47 mm lens and a macro Red DSMC2 Helium 8K Nikon ED 70–180 mm F4.5–5.6D. One submersible (Neptune) was equipped with a CTD probe, two parallel-aligned scaling lasers providing 100 mm scale, and a Schilling T4 hydraulic manipulator that was used for sampling activities. Video transects from Neptune were conducted using an ArcticRays Eagle Ray 4K camera recorded to a 4K Atmos Shogun monitor.

Stylasterid colonies were collected at three sampling stations in the northern Saudi Arabian Red Sea, namely NTN0029, NTN0048, and NTN0049 (Figure 1), in a bathymetric range spanning 166 to 492 m deep. After collection, colonies were air-dried at room temperature, and, for two colonies, small fragments were fixed in 99% ethanol. The specimens were firstly observed and photographed using a Leica M205 A stereomicroscope equipped with a Leica DMC 5004 camera in the Red Sea Research Center at King Abdullah University of Science and Technology (KAUST, Thuwal, Saudi Arabia) to assess their general macro-morphology. Subsequently, skeletal fragments were analyzed using a Thermo Fisher Scientific Quattro S Environmental scanning electron microscope (SEM) at KAUST Imaging Core Lab to describe the skeletal structures and using a Zeiss Axioskop 40 compound microscope equipped with a Canon PowerShot G7 X Mark II camera to study the cnidome composition. Specifically, for SEM fine-scale characterization of the skeletal structures, tissues were removed from dry specimens by immersion in a 10% sodium hypochlorite solution for 6–12 h. Skeletons were then rinsed, air-dried, and sputter-coated with Au–Pd. For cnidome characterization, the skeleton of ethanol-fixed fragments was dissolved by immersion in a 10% hydrochloric acid solution for 2–4 h, and the remaining tissues were washed with MilliQ water and directly observed under the compound microscope. All measurements were taken using the ImageJ 1.52p software [41]. The video footage obtained during the sampling campaign was also explored with the open-source software MPC-HC (Media Player Classic Home Cinema) available at <https://github.com/mpc-hc/mpc-hc> (accessed on 1 October 2021) to find other possible sites where stylasterids were present.

Two ethanol-fixed specimens were used for genomic DNA extraction with the DNeasy Blood and Tissue Kit (Qiagen: Hilden, Germany). Three molecular markers were amplified using polymerase chain reactions (PCRs) following Lindner et al. [36]. Specifically, a ~600 bp portion of the mitochondrial 16S ribosomal DNA (16S rRNA) was amplified using the primers SHB–SHA and protocols in Cunningham and Buss [42], a ~1600 bp portion of the nuclear 18S ribosomal DNA (18S rRNA) was amplified using the primers 18SA–18SB and protocols in Medlin et al. [43], and a ~350 bp portion of the nuclear calmodulin gene (CaM) was amplified using the primers CAMF1–CAMR1 and protocols in Lindner et al. [36]. All PCR products were checked using a QIAxcel Capillary Electrophoresis System (Qiagen: Hilden, Germany), purified with Illustra ExoStar (GE Healthcare: Amersham, UK), and sequenced in forward and reverse directions using an ABI 3730xl DNA Analyzer (Applied Biosystems: Carlsbad, CA, USA) at KAUST Bioscience Core Lab. Geneious 7.1.9 (Biomatters Ltd.: Auckland, New Zealand) was used to visually check and assemble the obtained chromatograms, and the consensus sequences were deposited in GenBank with the accession numbers OM416034, OM416035, OM416037, and OM416038.

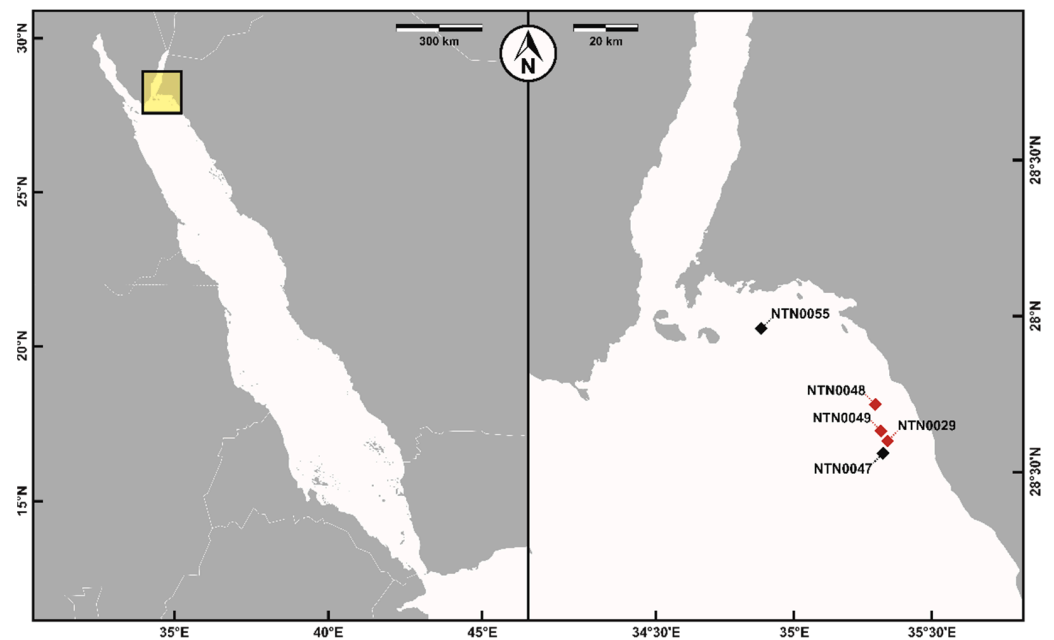


Figure 1. Map showing the sampling localities. Red diamonds show sites where samples were collected, while black diamonds show sites where samples were only observed.

Sequences of each DNA region were aligned using MAFFT 7.110 [44] with the E-INS-i option, after adding other available stylasterid sequences and outgroups listed in Lindner et al. [36,45] and after updating species names following Cairns [40] and Cairns and Lindner [46]. The 16S and 18S rRNA datasets were run through Gblocks [47,48] using the default ‘less stringent’ settings to remove ambiguously aligned regions (~9% and ~2% of the alignments, respectively), and all datasets were concatenated using Mesquite 3.2 [49], resulting in a final alignment of 2583 bp. Partition schemes and models for the concatenated dataset were determined with PartitionFinder 1.1.1 [50] using the Akaike information criterion, resulting in partitioning by DNA region and applying the GTR + I + G model to all partitions. Phylogenetic inference was performed using maximum likelihood (ML), maximum parsimony (MP), and Bayesian inference (BI) with RAxML 8.2.12 [51], PAUP 4.0b10 [52], and MrBayes 3.2.6 [53], respectively, as described in Maggioni et al. [54].

The holotype was deposited at the Museo Civico di Storia Naturale, Cnidaria Collection, Milano, Italy, whereas the paratypes at the KAUST. The acronyms for the voucher and deposited material are MSNM-Coe-# (Museo Civico di Storia Naturale, Cnidaria Collection, Milano, Italy) and NTN-# (Neptune).

3. Results

3.1. Sampling and Phylogenetic Analyses

The sampled colonies belonged to the genus *Stylaster*, representing the first record of a deep-sea stylasterid, as well as the first record of the genus *Stylaster*, in the Red Sea. According to morphological and molecular analyses (Figure 2), the collected colonies resulted to be conspecific and to belong to *Stylaster tritoni* sp. nov. (see Section 3.2), a previously unknown species.

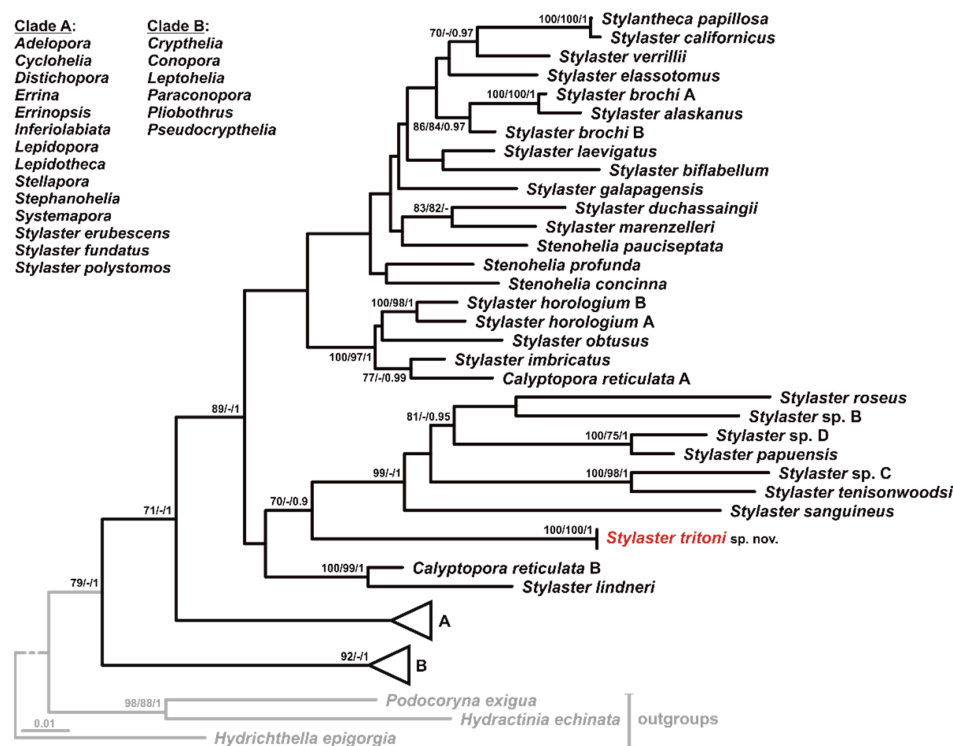


Figure 2. Phylogenetic hypothesis of the Stylasteridae based on the concatenated dataset, with *Stylaster tritoni* sp. nov. in red. The tree topology reflects the ML analysis and numbers at nodes show ML bootstrap values, MP bootstrap values, and Bayesian posterior probabilities, respectively; they are shown only when at least two analyses resulted in support values ≥ 70 (ML and MP) or ≥ 0.9 (BI). Species represented only by letters follow identifications of Lindner et al. [36]. Representatives of clades A and B are listed in the legend.

PCRs and sequencing were successful for 16S and 18S rRNA, but not for the CaM gene, and the phylogenetic analyses confirmed that *S. tritoni* sp. nov. was genetically different from any stylasterid species sequenced so far. Specifically, the obtained phylogenetic hypotheses (Figure 2) were comparable to those reported by previous studies [36,45]. Similar to previous phylogenetic reconstructions, deeper nodes within the Stylasteridae family were generally not well supported, and the genus *Stylaster* as currently defined is polyphyletic. *Stylaster tritoni* sp. nov. sequences formed a fully supported monophyletic group, sister to a clade composed of shallow-water *Stylaster* species inhabiting tropical Indo-Pacific waters, apart from *Stylaster roseus* (Pallas, 1776) from the tropical Western Atlantic [36]. This latter clade, together with *S. tritoni* sp. nov., formed a clade sister to two deep-sea species from the West Pacific, *Stylaster lindneri* Cairns, 2015 and *Calyptopora reticulata* B (identified as *Stylaster* cf. *horologium* and *Calyptopora sinuosa* Cairns, 1991, respectively, in Lindner et al. [36]). All other *Stylaster* species included in the analyses clustered in two divergent clades, together with species belonging to several other stylasterid genera.

3.2. Taxonomic Account

Class: Hydrozoa (Owen, 1843)

Order: Anthoathecata (Cornelius, 1992)

Family: Stylasteridae (Gray, 1847)

Genus: *Stylaster* (Gray, 1831)

Stylaster tritoni sp. nov. Maggioni, Cairns, Pica & Benzoni

urn:lsid:zoobank.org:act:194FD2C1-8FEC-4611-AA4E-07B5A9C20B31.

Type material: NTN0048-7 (Holotype): one dry colony and fragments from the same colony in 99% ethanol, station NTN0048, 27.71701° N 35.28974° E, 373 m, 1 November 2020,

GenBank accession numbers: OM416035 (16S rRNA), OM416038 (18S rRNA). Voucher number: MSNM-Coe-356.

Additional examined material: NTN0029-5: one dry colony and fragments from the same colony in 99% ethanol, station NTN0029, 27.60023° N 35.33427° E, 492 m, 10 October 2020, GenBank accession numbers: OM416034 (16S rRNA), OM416037 (18S rRNA); NTN0029-19: one dry colony, station NTN0029, 27.58968° N 35.33203° E, 166 m, 10 October 2020; NTN0049-1: one dry colony, station NTN0049, 27.63267° N 35.31033° E, 166 m, 1 November 2020.

Description: Corallum uniplanar or slightly multiplanar in larger colonies, thin, delicate, and highly branched (Figures 3 and 4A–C). Holotype ~17 cm in height and ~28 cm in width, with a basal branch diameter of ~1 cm (Figures 3A,B and 4A). Other investigated colonies smaller (Figure 4B–D). Branching generally dichotomous, rarely anastomosing in certain points. Main branches ~3 mm in diameter and other branches thinner, ~1 mm in diameter, terminating in a terminal cyclosystem (Figure 4E). Commensal organisms not observed. Coenosteal texture linear-imbricate (Figure 5A), with strips 47–140 µm wide and slightly ridged, especially in smaller branches (Figure 4G), and slits 43–97 µm wide. Texture becomes more irregular and granular in some points and in larger branches (Figure 5C). Platelets with normal polarity, 52–136 µm wide and 11–27 µm high (Figure 5A,B), each one extending entirely across strips and with edges irregular in shape. Coenosteal pores round to slightly elliptical in shape, 14–36 µm in diameter, with (Figure 5C) or without (Figure 5A) small teeth, 5–18 µm in length, projecting inward toward center of pore; teeth observed when texture is more irregular and granular. Coenosteal pores in larger branches more scattered than longitudinally organized in slits (Figure 5E). Conical nematopores present on some of the main and smaller branches (Figure 5D–F), up to 50 µm in height, with apical pore measuring 67–94 µm in diameter. Living colonies uniformly white (Figure 4A–D).

Cyclosystems sympodially arranged, circular to slightly elliptical in outline, with no diastemas, ranging from 0.5–1.0 mm in diameter, with terminal ones being slightly smaller (0.5–0.8 mm in diameter) (Figures 4E,F and 5G–I). Average number of dactylopores per cyclosystem: 12.0 ($n = 50$, range = 7–16, standard deviation = ± 1.6 , mode = 12).

Gastropores circular, 0.19–0.34 mm in diameter (Figure 5G–J), leading to cylindrical gastropore tubes (Figure 5K). Gastrostyles generally not visible from surface, cylindrical, with slightly pointed end (Figure 5J,L–N), 0.27–0.37 mm long and 54–94 µm in diameter. Gastrostyles not ridged, with spines often multi-tipped (Figure 5O,P), 8–32 µm long. Annular ring palisade at level of gastrostyle tip, composed of 3–4 rings of cylindrical to clavate elements (Figures 5J,K,M,N and 6A,B), 14–46 µm in length and 8–19 µm in diameter. Dactylopores round to elliptical, dactylotomes measuring 44–107 µm in width (Figure 5G–J), triangular pseudosepta 43–177 µm wide. Older cyclosystems with absent or reduced dactylotomes, generally reducing dactylopores diameter (Figure 5I). Dactylostyles generally absent. Occasionally, in some dactylopores of terminal cyclosystems, small protruding elements 6–14 µm high occur in uppermost part of dactylopores tubes (Figure 5J), resembling dactylostyle elements.

External female ampullae mostly observed on smaller branches (Figures 4F and 6C–F), 0.44–0.68 mm in diameter, with a lateral efferent pore (Figure 6D–F), 77–132 µm in diameter. Male ampullae not observed.

Cnidome composed of three types of nematocysts concentrated in dactylozooids and gastrozooids, but also scattered in the coenosarc: desmonemes (3–4 × 2–3 µm) (Figure 7A), large microbasic euryteles (9–10 × 4–6 µm; shaft: 8) (Figure 7A,B), small microbasic euryteles (5–8 × 2–3 µm; shaft: 5 µm) (Figure 7A,C).

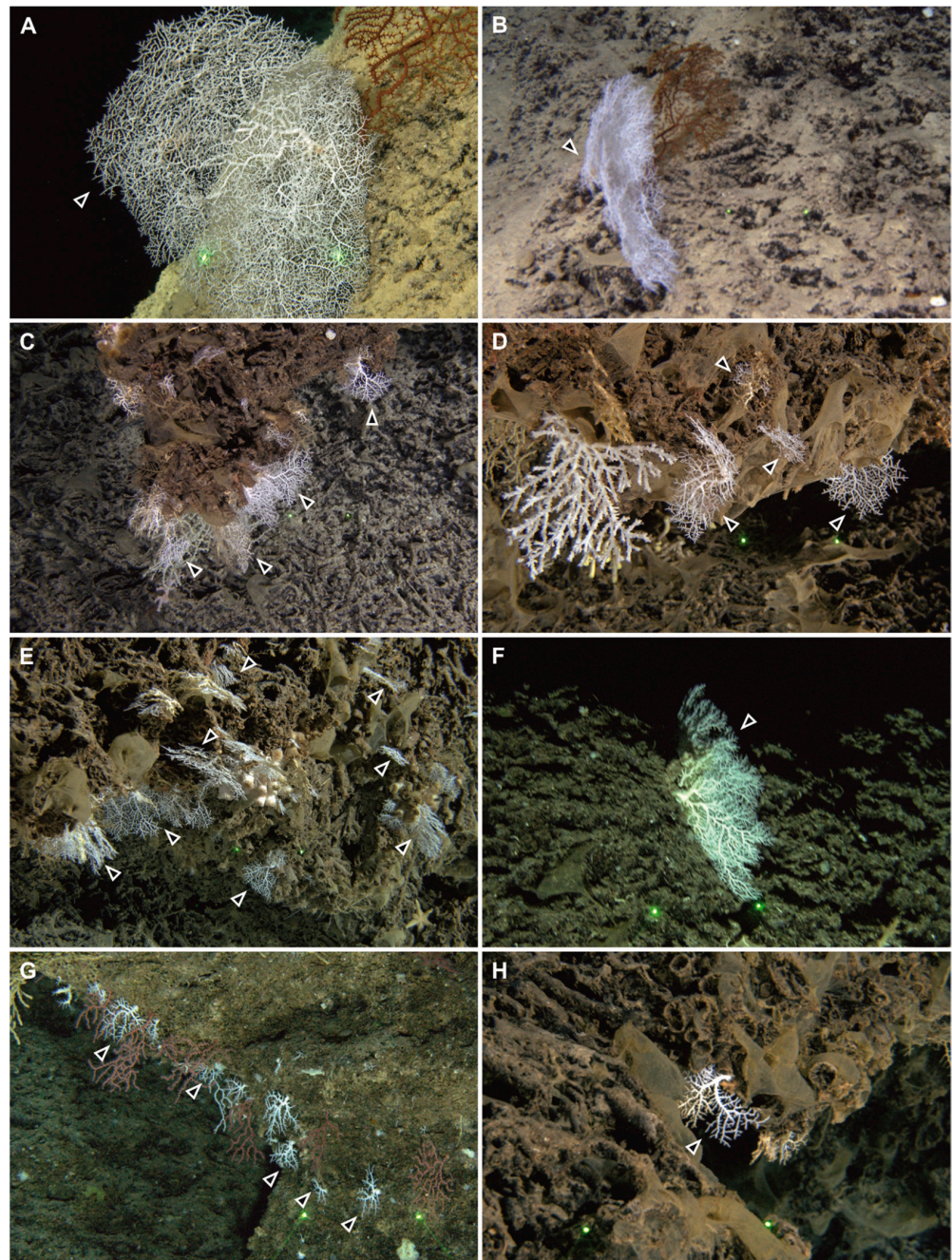


Figure 3. In situ photographs of *Stylaster tritoni* sp. nov. (A,B) Largest observed colony (holotype) in frontal and lateral view, respectively, and associated with a gorgonian. (C–H) Photographs showing the habitat and aggregations of *S. tritoni* sp. nov., commonly associated with living scleractinians and octocorals. Arrowheads indicate stylasterid colonies. The distance between the two green laser points indicates 10 cm.

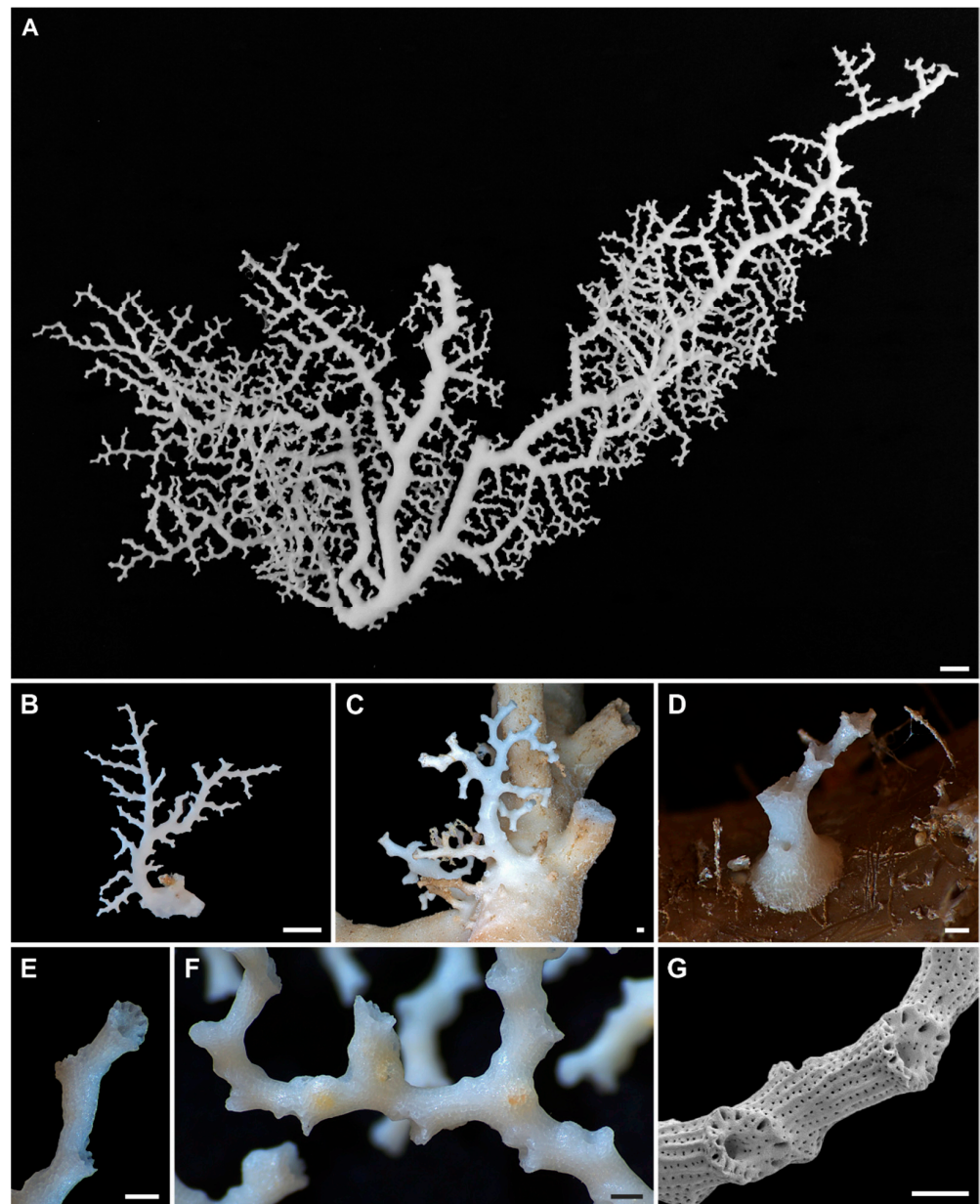


Figure 4. Corallum of *Stylaster tritoni* sp. nov. (A) Portion of the colony figured in Figure 3A,B (holotype) and (B–D) other collected colonies (paratypes). Colonies in (C) and (D) growing on a dead dendrophylliid scleractinian and a dead portion of a gorgonian, respectively. Detailed view of the (E) cyclosystem on a terminal branch and (F) female ampullae of the holotype. (G) Terminal branch of the holotype showing the longitudinal lines of coenosteal pores and slightly ridged strips. Scale bars: (A,B) 5 mm, (C–G) 0.5 mm.

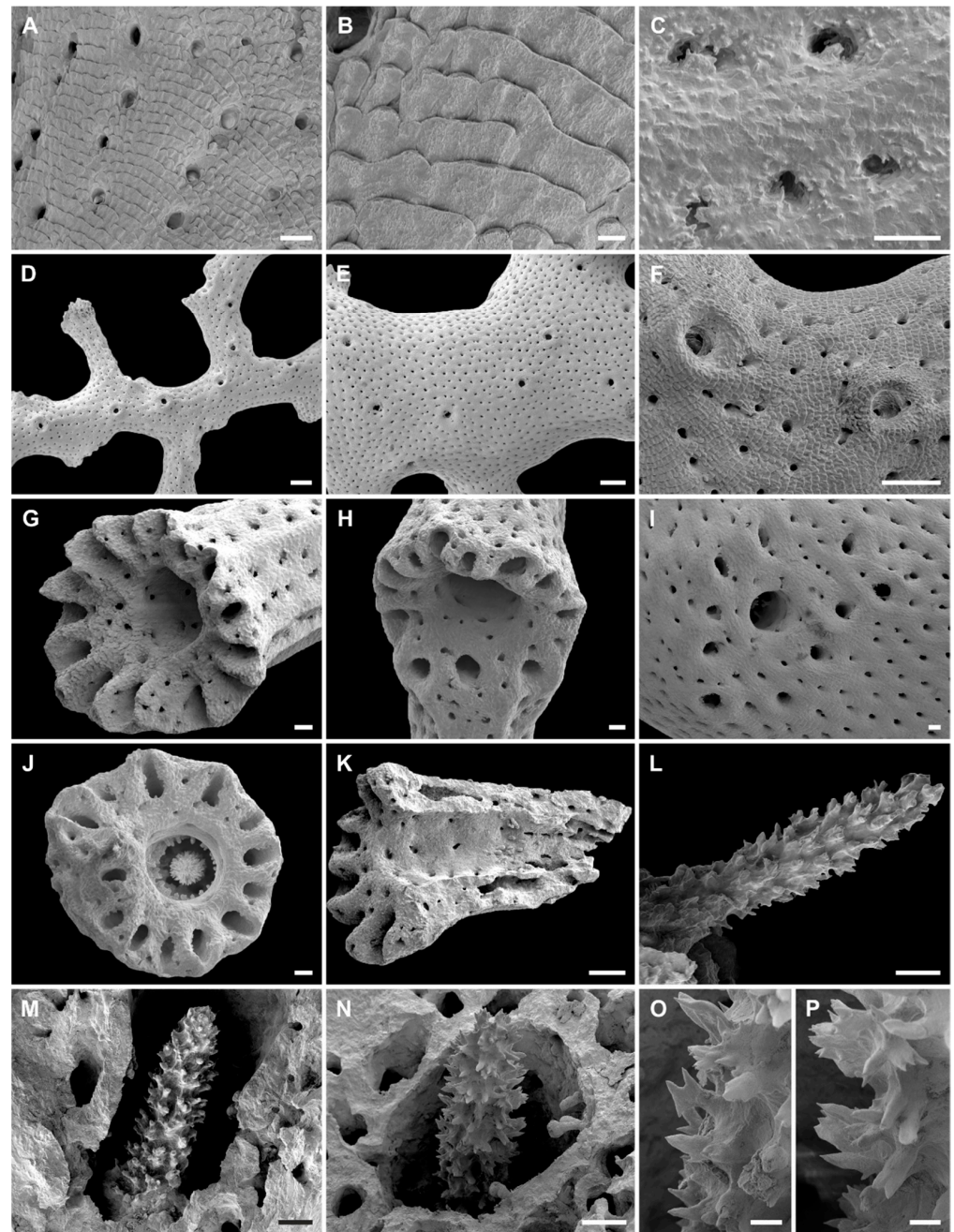


Figure 5. Texture, cyclostyles, and gastrostyles of *Stylaster tritoni* sp. nov. (holotype). (A) Linear-imbricate coenosteal texture and (B) detail of platelets. (C) Portion with a more irregular and granular imbricate texture, showing pores with teeth. (D) Branch showing nematopores and (E) larger branch with a more scattered pore distribution and nematopores. (F) Detailed view of two nematopore mounds. (G) Terminal cyclostyle, (H) Cyclostyle on a small branch, and (I) cyclostyle on a large branch. (J) Stereo view of a terminal cyclostyle and (K) longitudinal section of a terminal cyclostyle. (L–N) Gastrostyles and (O,P) details of their spines. Scale bars: (A,C,G–N) 50 μm ; (B,O,P) 10 μm ; (D,E) 300 μm ; (F) 30 μm .

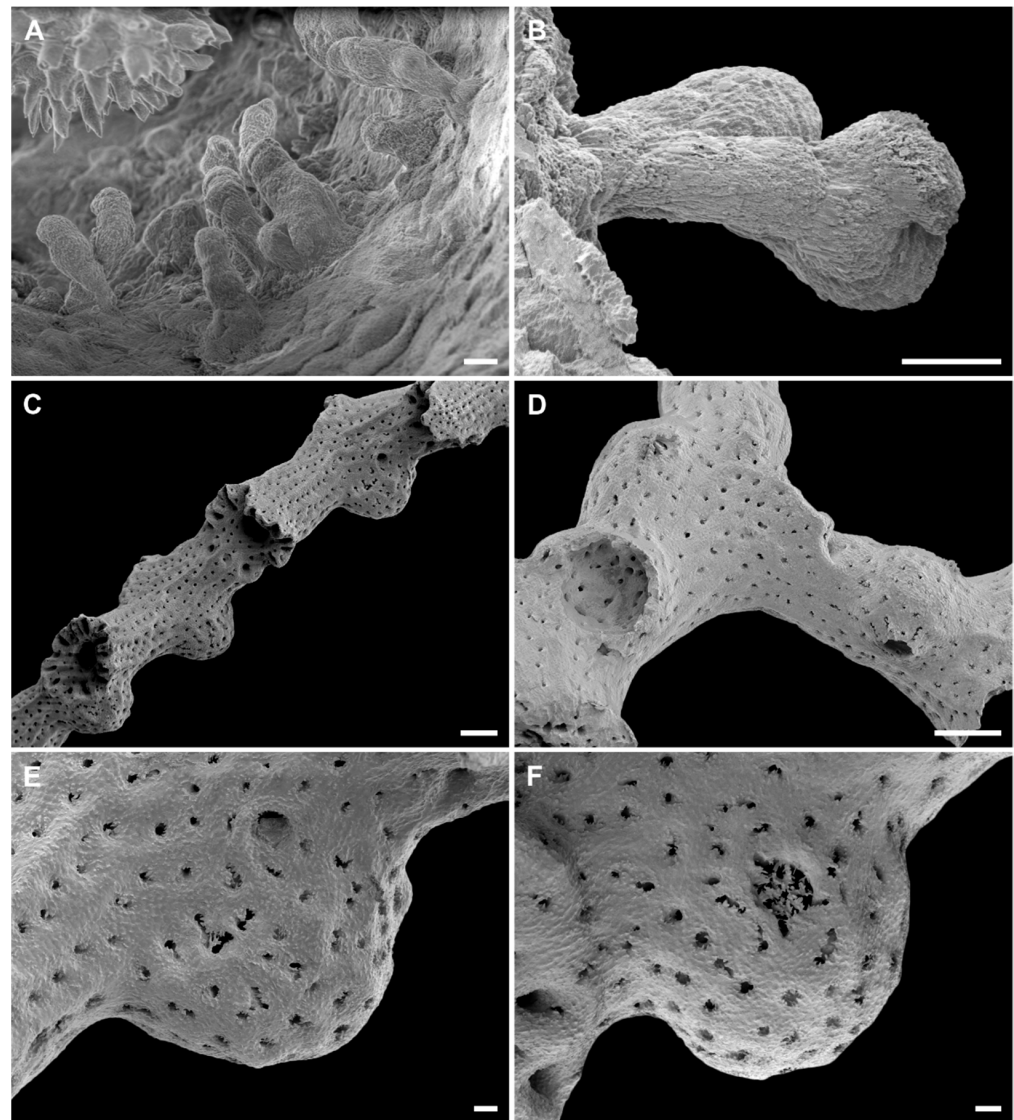


Figure 6. Ring palisade, dactylostyles, and ampullae of *Stylaster tritoni* sp. nov. (holotype). (A) Ring palisade and (B) detailed view of a clavate element. (C) Female ampullae on a small branch. (D) A broken ampulla (left side) and an intact one showing a large efferent pore (right side). (E,F) Detailed view of two female ampullae with efferent pores. Scale bars: (A,B) 10 μm ; (C,D) 300 μm ; (E,F) 50 μm .

Habitat: *Stylaster tritoni* sp. nov. was commonly found in aggregations close to other cnidarians, including scleractinians and octocorals, and growing on dendrophylliid and caryophylliid rubble (Figures 3 and 4C). Moreover, it was observed both growing directed upward and downward (Figure 3).

Distribution: Known only from the type locality (northern Saudi Arabian Red Sea). Bathymetric range: 166–492 m. Samples observed in situ but not collected were found at the following stations and depths: NTN0047, 27.56355° N 35.32176° E, 242–271 m, 31 October 2020; NTN0049, 27.63267° N 35.31033° E, 400–414 m, 1 November 2020; NTN0055, 27.95855° N 34.87867° E, 272–276 m, 6 November 2020 (Figure 1).

Etymology: The specific name derives from Triton, a god of the sea in Greek mythology, son of Poseidon and Amphitrite, the god and goddess of the sea, respectively. Triton is also the name of the submersibles used to collect and photograph the species.

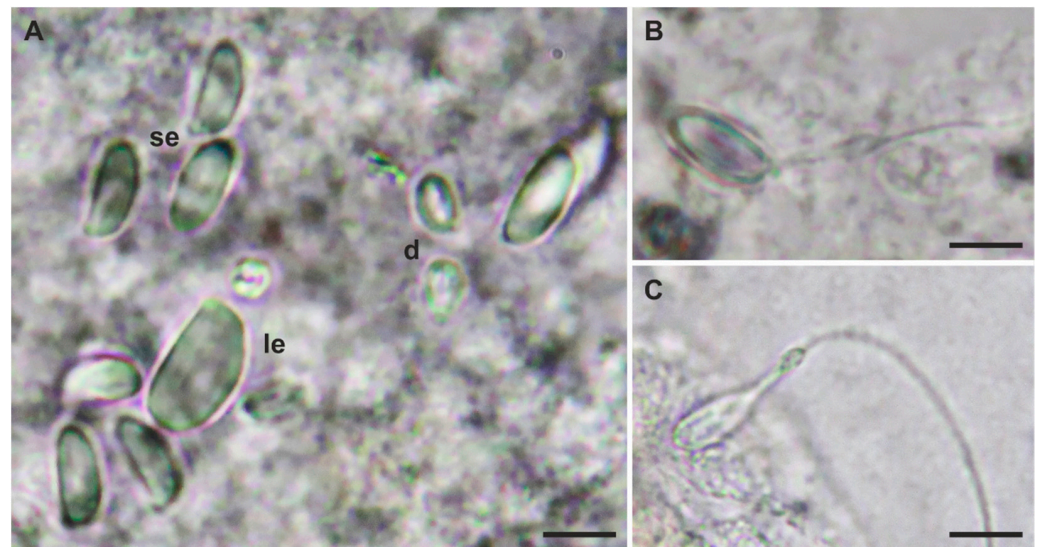


Figure 7. Cnidome of *Stylaster tritoni* sp. nov. (holotype). (A) Undischarged desmonemes (d), small euryteles (se), large eurytele (le). Discharged (B) large eurytele and (C) small eurytele. Scale bars: (A–C) 5 μ m.

Remarks: *Stylaster tritoni* sp. nov. belongs to the ‘*Stylaster Group C*’ *sensu* Cairns [55], by having cyclosystems exclusively arranged in a sympodial fashion on branch edges and branches ending in a terminal cyclo-system. *Stylaster tritoni* sp. nov. is the only species in the genus and only the second stylasterid species reported from the Red Sea after *Distichopora violacea* [34], supporting its description as a new species, given the overall limited distributional ranges of stylasterids [39]. Three other *Stylaster C* species are known to inhabit the Indian Ocean, namely, *Stylaster lonchitis* Broch, 1947, *Stylaster ramosus* Broch, 1947, and *Stylaster flabelliformis* (Lamarck, 1816). The first two species were reported from the Pemba Channel (Tanzania) [56], whereas the latter was reported from Mascarene Islands [57]. *Stylaster lonchitis* differs from *S. tritoni* sp. nov. by having diastemas, distinct dactylostyles, and highly corrugated ampullae; conversely, *S. ramosus* is more similar to the Red Sea species but can be mostly distinguished by a lower number of dactylopores per cyclo-system (average 8.94). Lastly, *S. flabelliformis* resembles *S. tritoni* sp. nov., showing nevertheless a more uniplanar corallum, with platelets of the texture not long as the strip, sometimes spines on ampullae and coenosteum, dactylopores in older cyclo-systems elliptical (circular in *S. tritoni* sp. nov.), and no nematopores. Moreover, *S. flabelliformis* has rudimentary linear dactylostyles, whereas *S. tritoni* sp. nov. does not show this feature.

4. Discussion

Stylaster is the most species-rich genus in the family Stylasteridae, and among the richest in the whole phylum Cnidaria. With the description of *Stylaster tritoni* sp. nov., the number of the extant accepted species of the genus rises to 91 [58]. Altogether, stylasterids account for about 10% of the known hydrozoan species [58], and their high diversity may be explained by the fact that they are the only calcifying hydrozoans in the deep sea, also resulting in great adaptive advantages in terms of protection of polyps, ability to reach a large size, and reduced competition [40]. This idea is also supported by the fact that the highest stylasterid diversity is found in deep waters [35].

With this work, we extend the known geographic distribution of the genus *Stylaster*, since no previous records in the Red Sea were available in the literature. A few other *Stylaster* species are known from the Western Indian Ocean, such as the ‘Group A’ *Stylaster omanensis* Cairns & Samimi-Namin, 2015, or the ‘Group C’ *Stylaster flabelliformis*, *Stylaster lonchitis*, and *Stylaster ramosus* [56,57,59], whereas most of the species inhabit the Atlantic and Pacific Oceans. Additionally, another unidentified *Stylaster* species was collected in the

Gulf of Aden during the Meteor Expedition in 1987 (st. 230, 228–235 m), but no detailed morphological information is currently available to precisely determine the species (H. Zibrowius and D. Pica, personal observation). Stylasterid species generally have narrow distributional ranges [39,60], possibly explained by the ecological preferences [39] and the poor dispersal abilities of the larvae [61], resulting in high levels of endemism. Miller et al. [62] demonstrated, for instance, that neighboring populations of *Errina novaeseelandiae* Hickson, 1912 in New Zealand fjords were characterized by limited gene flow and low levels of heterozygosity, typical of organisms with limited dispersal abilities. In this context, *Stylaster tritoni* sp. nov. may be a Red Sea or even northern Red Sea endemic. Indeed, this basin is characterized by multiple dispersal barriers, including its narrow entrance and heterogeneous salinity, temperature, and primary productivity. These conditions isolate it from adjacent waters and create longitudinal environmental gradients [17,19,63], resulting in genetic breaks among populations (e.g., [64–66]) and high levels of endemism [17], as demonstrated by the constant discovery of species only found in the Red Sea (e.g., [67–69]). These features, together with the abovementioned reproductive traits of stylasterid species, may indicate a restricted distribution of *S. tritoni*, but further deep-sea explorations of the Red Sea and neighboring waters are needed to address whether *S. tritoni* is a Red Sea endemic or not.

The stylasterid genetic diversification patterns were examined by Lindner et al. [36] using three molecular markers, who obtained phylogenetic reconstructions highlighting the strong need of an integrative systematic revision of the family [70]. Indeed, many genera resulted polyphyletic, with low statistical support at nodes, as also observed in our phylogenetic hypotheses. Therefore, it is fundamental to increase the sampling effort in terms of number of samples and geographic coverage, as well as the amount of genetic data. In turn, a detailed genetic characterization of this taxon will enhance our knowledge about the diversity, evolution, and biogeography of stylasterids, contributing toward the development of effective conservation measures for such a peculiar and ecologically important group of hydrozoans.

Author Contributions: Conceptualization, F.B.; sampling, G.C., T.I.T., F.M. and F.B.; investigation, D.M., T.I.T., D.P. and S.D.C.; writing—original draft preparation, all authors; writing—review and editing, all authors. All authors have read and agreed to the published version of the manuscript.

Funding: This work was supported by KAUST (FCC/1/1973-50-01, FCC/1/1973-49-01, and baseline research funds to F. Benzoni). G. Chimienti was supported by the Italian Ministry of Education, University and Research (PON 2014–2020, Grant AIM 1807508-1, Linea 1).

Data Availability Statement: Not applicable.

Acknowledgments: This research was undertaken in accordance with the policies and procedures of the King Abdullah University of Science and Technology (KAUST). Permission relevant for KAUST to undertake the research was obtained from the applicable governmental agencies in the Kingdom of Saudi Arabia. We would like to thank OceanX and the crew of OceanXplorer for their operational and logistical support for the duration of the expedition. In particular, we would like to acknowledge the ROV and submersible teams for data acquisition and sample collection, and the OceanXplorer crew for support of scientific operations on board. We would also like to thank OceanX Media for documenting and communicating the work with the public. We finally thank two anonymous reviewers whose comments improved the manuscript.

Conflicts of Interest: The authors declare no conflict of interest.

References

1. Roberts, J.M.; Wheeler, A.J.; Freiwald, A.; Cairns, S.D. *Cold-Water Corals: The Biology and Geology of Deep-Sea Coral Habitats*; Cambridge University Press: Cambridge, UK, 2009; ISBN 978-051-158-158-8.
2. Rex, M.A.; Etter, R.J. *Deep-Sea Biodiversity: Pattern and Scale*; Harvard University Press: Cambridge, MA, USA, 2010; ISBN 978-067-403-607-9.
3. Danovaro, R.; Snelgrove, P.V.; Tyler, P. Challenging the paradigms of deep-sea ecology. *Trends Ecol. Evol.* **2014**, *29*, 465–475. [[CrossRef](#)] [[PubMed](#)]

4. Angeletti, L.; Taviani, M.; Canese, S.; Fogliani, F.; Mastrototaro, F.; Argnani, A.; Trincarrdi, F.; Bakran-Petricioli, T.; Ceregato, G.; Chimienti, G.; et al. New deep-water cnidarian sites in the southern Adriatic Sea. *Mediterr. Mar. Sci.* **2014**, *15*, 263–273. [[CrossRef](#)]
5. Chimienti, G.; Aguilar, R.; Gebruk, A.V.; Mastrototaro, F. Distribution and swimming ability of the deep-sea holothuroid *Penilpidia ludwigi* (Holothuroidea: Elaspodida: Elpidiidae). *Mar. Biodivers.* **2019**, *49*, 2369–2380. [[CrossRef](#)]
6. Chimienti, G.; Angeletti, L.; Furfaro, C.; Taviani, M. Habitat, morphology and trophism of *Tritonia callogorgiae* sp. nov., a large nudibranch inhabiting *Callogorgia verticillata* forests in the Mediterranean Sea. *Deep Sea Res. I Oceanogr. Res. Pap.* **2020**, *165*, 103364. [[CrossRef](#)]
7. Friedlander, A.M.; Giddens, J.; Ballesteros, E.; Blum, S.; Brown, E.K.; Caselle, J.E.; Henning, B.; Jost, C.; Salinas-de-Léon, P.; Sala, E. Marine biodiversity from zero to a thousand meters at Clipperton Atoll (Île de La Passion), Tropical Eastern Pacific. *PeerJ* **2019**, *7*, e7279. [[CrossRef](#)]
8. Augustin, N.; van der Zwan, F.M.; Devey, C.W.; Brandsdóttir, B. 13 million years of seafloor spreading throughout the Red Sea Basin. *Nat. Commun.* **2021**, *12*, 2427. [[CrossRef](#)]
9. Berumen, M.L.; Voolstra, C.R.; Daffonchio, D.; Agusti, S.; Aranda, M.; Irigoien, X.; Jones, B.H.; Morán, X.A.G.; Duarte, C.M. The Red Sea: Environmental gradients shape a natural laboratory in a nascent ocean. In *Coral Reefs of the Red Sea*; Voolstra, C.R., Berumen, M.L., Eds.; Springer: Cham, Switzerland, 2019; pp. 1–10. ISBN 978-303-005-802-9.
10. Sheppard, C.; Price, A.; Roberts, C. *Marine Ecology of the Arabian Region: Patterns and Processes in Extreme Tropical Environments*; Academic Press: London, UK, 1992; ISBN 978-012-639-490-0.
11. Roder, C.; Berumen, M.L.; Bouwmeester, J.; Papathanassiou, E.; Al-Suwailam, A.; Voolstra, C.R. First biological measurements of deep-sea corals from the Red Sea. *Sci. Rep.* **2013**, *3*, 2802. [[CrossRef](#)]
12. Qurban, M.A.; Krishnakumar, P.K.; Joydas, T.V.; Manikandan, K.P.; Ashraf, T.T.M.; Quadri, S.I.; Wafar, M.; Qasem, A.; Cairns, S.D. In-situ observation of deep water corals in the northern Red Sea waters of Saudi Arabia. *Deep-Sea Res. I Oceanogr. Res. Pap.* **2014**, *89*, 35–43. [[CrossRef](#)]
13. Riegl, B.M.; Bruckner, A.W.; Rowlands, G.P.; Purkis, S.J.; Renaud, P. Red Sea coral reef trajectories over 2 decades suggest increasing community homogenization and decline in coral size. *PLoS ONE* **2012**, *7*, e38396. [[CrossRef](#)]
14. Berumen, M.L.; Hoey, A.S.; Bass, W.H.; Bouwmeester, J.; Catania, D.; Cochran, J.E.M.; Khalil, M.T.; Miyake, S.; Mughal, M.R.; Spaet, J.L.Y.; et al. The status of coral reef ecology research in the Red Sea. *Coral Reefs* **2013**, *32*, 737–748. [[CrossRef](#)]
15. Loya, Y.; Genin, A.; El-Zibdeh, M.; Naumann, M.S.; Wild, C. Reviewing the status of coral reef ecology of the Red Sea: Key topics and relevant research. *Coral Reefs* **2014**, *33*, 1179–1180. [[CrossRef](#)]
16. Rowlands, G.; Purkis, S.; Bruckner, A. Tight coupling between coral reef morphology and mapped resilience in the Red Sea. *Mar. Pollut. Bull.* **2016**, *105*, 575–585. [[CrossRef](#)] [[PubMed](#)]
17. DiBattista, J.D.; Roberts, M.B.; Bouwmeester, J.; Bowen, B.W.; Coker, D.J.; Lozano-Cortés, D.F.; Choat, J.H.; Gaither, M.R.; Hobbs, J.-P.A.; Khalil, M.T.; et al. A review of contemporary patterns of endemism for shallow water reef fauna in the Red Sea. *J. Biogeogr.* **2016**, *43*, 423–439. [[CrossRef](#)]
18. Berumen, M.L.; Arrigoni, R.; Bouwmeester, J.; Terraneo, T.I.; Benzoni, F. Corals of the Red Sea. In *Coral Reefs of the Red Sea*; Voolstra, C.R., Berumen, M.L., Eds.; Springer: Cham, Switzerland, 2019; pp. 123–155. ISBN 978-303-005-802-9.
19. DiBattista, J.D.; Howard Choat, J.; Gaither, M.R.; Hobbs, J.-P.A.; Lozano-Cortés, D.F.; Myers, R.F.; Paulay, G.; Rocha, L.A.; Toonen, R.J.; Westneat, M.W.; et al. On the origin of endemic species in the Red Sea. *J. Biogeogr.* **2016**, *43*, 13–30. [[CrossRef](#)]
20. Joydas, T.V.; Manokaran, S.; Borja, A.; Rabaoui, L.; Manikandan, K.P.; Ashraf, T.T.M.; Aarif, K.M.; Hussain, S.A.; Baig, M.H.; Shoeb, M.; et al. A baseline quantitative assessment of deep-sea benthic fauna of the Gulf of Aqaba (Northern Saudi Arabia, Red Sea). *Mar. Pollut. Bull.* **2021**, *164*, 112028. [[CrossRef](#)]
21. Gravili, C.; Di Camillo, C.G.; Piraino, S.; Boero, F. Hydrozoan species richness in the Mediterranean Sea: Past and present. *Mar. Ecol.* **2013**, *34*, 41–62. [[CrossRef](#)]
22. Pica, D.; Bastari, A.; Vaga, C.F.; Di Camillo, C.G.; Montano, S.; Puce, S. Hydroid diversity of Eilat Bay with the description of a new *Zanclaea* species. *Mar. Biol. Res.* **2017**, *13*, 469–479. [[CrossRef](#)]
23. Maggioni, D.; Montano, S.; Arrigoni, R.; Galli, P.; Puce, S.; Pica, D.; Berumen, M.L. Genetic diversity of the *Acropora*-associated hydrozoans: New insight from the Red Sea. *Mar. Biodivers.* **2017**, *47*, 1045–1055. [[CrossRef](#)]
24. Maggioni, D.; Schiavo, A.; Ostrovsky, A.N.; Seveso, D.; Galli, P.; Arrigoni, R.; Francesca, B.; Montano, S. Cryptic species and host specificity in the bryozoan-associated hydrozoan *Zanclaea divergens* (Hydrozoa, Zanclaeidae). *Mol. Phylogenet. Evol.* **2020**, *151*, 106893. [[CrossRef](#)]
25. Maggioni, D.; Arrigoni, R.; Seveso, D.; Galli, P.; Berumen, M.L.; Denis, V.; Hoeksema, B.W.; Huang, D.; Manca, F.; Pica, D.; et al. Evolution and biogeography of the *Zanclaea*-Scleractinia symbiosis. *Coral Reefs* **2020**, 1–17. [[CrossRef](#)]
26. Maggioni, D.; Schuchert, P.; Arrigoni, R.; Hoeksema, B.W.; Huang, D.; Strona, G.; Seveso, D.; Berumen, M.L.; Montalbetti, E.; Collins, R.; et al. Integrative systematics illuminates the relationships in two sponge-associated hydrozoan families (*Capitata: Sphaerocorynidae* and *Zanclaeopsidae*). *Contr. Zool.* **2021**, *90*, 487–525. [[CrossRef](#)]
27. Dayrat, B. Towards integrative taxonomy. *Biol. J. Linn. Soc.* **2005**, *85*, 407–417. [[CrossRef](#)]
28. Randall, J.E.; DiBattista, J.D. A new species of damselfish (*Pomacentridae*) from the Indian Ocean. *AQUA* **2013**, *19*, 1–16.
29. Voigt, O.; Erpenbeck, D.; González-Pech, R.A.; Al-Aidaros, A.M.; Berumen, M.L.; Wörheide, G. Calcinea of the Red Sea: Providing a DNA barcode inventory with description of four new species. *Mar. Biodivers.* **2017**, *47*, 1009–1034. [[CrossRef](#)]

30. Perry, O.; Bronstein, O.; Simon-Blecher, N.; Atkins, A.; Kupriyanova, E.; ten Hove, H.; Levy, O.; Fine, M. On the genus *Spirobranchus* (*Annelida, Serpulidae*) from the northern Red Sea, and a description of a new species. *Invertebr. Syst.* **2018**, *32*, 605–626. [[CrossRef](#)]
31. Loya, Y. Community structure and species diversity of hermatypic corals at Eilat, Red Sea. *Mar. Biol.* **1972**, *13*, 100–123. [[CrossRef](#)]
32. Perkol-Finkel, S.; Benayahu, Y. Community structure of stony and soft corals on vertical unplanned artificial reefs in Eilat (Red Sea): Comparison to natural reefs. *Coral Reefs* **2004**, *23*, 195–205. [[CrossRef](#)]
33. Arrigoni, R.; Maggioni, D.; Montano, S.; Hoeksema, B.W.; Seveso, D.; Shlesinger, T.; Terraneo, T.I.; Tietbohl, M.D.; Berumen, M.L. An integrated morpho-molecular approach to delineate species boundaries of *Millepora* from the Red Sea. *Coral Reefs* **2018**, *37*, 967–984. [[CrossRef](#)]
34. Boschma, H. Revision of the Indo-Pacific species of the genus *Distichopora*. *Bijdr. Dierkd.* **1959**, *29*, 121–171. [[CrossRef](#)]
35. Cairns, S.D. Global diversity of the Stylasteridae (*Cnidaria: Hydrozoa: Athecatae*). *PLoS ONE* **2011**, *6*, e21670. [[CrossRef](#)]
36. Lindner, A.; Cairns, S.D.; Cunningham, C.W. From offshore to onshore: Multiple origins of shallow-water corals from deep-sea ancestors. *PLoS ONE* **2008**, *3*, e2429. [[CrossRef](#)] [[PubMed](#)]
37. Cairns, S.D. Deep-water corals: An overview with special reference to diversity and distribution of deep-water scleractinian corals. *Bull. Mar. Sci.* **2007**, *81*, 311–322.
38. Hoarau, L.; Rouzé, H.; Boissin, É.; Gravier-Bonnet, N.; Plantard, P.; Loisel, C.; Bigot, L.; Chabanet, P.; Labarrère, P.; Penin, L.; et al. Unexplored Refugia with High Cover of Scleractinian *Leptoseris* spp. and Hydrocorals *Stylaster flabelliformis* at Lower Mesophotic Depths (75–100 m) on Lava Flows at Reunion Island (Southwestern Indian Ocean). *Diversity* **2021**, *13*, 141. [[CrossRef](#)]
39. Cairns, S.D. Worldwide distribution of the Stylasteridae (*Cnidaria: Hydrozoa*). *Sci. Mar.* **1992**, *56*, 125–130.
40. Cairns, S.D. Stylasteridae (*Cnidaria: Hydrozoa: Anthoathecata*) of the New Caledonian Region. *Mém. Mus. Natl. Hist. Nat.* **2015**, *207*, 1–361.
41. Schneider, C.A.; Rasband, W.S.; Eliceiri, K.W. NIH Image to ImageJ: 25 years of image analysis. *Nat. Methods* **2012**, *9*, 671–675. [[CrossRef](#)]
42. Cunningham, C.W.; Buss, L.W. Molecular evidence for multiple episodes of paedomorphosis in the family *Hydractiniidae*. *Biochem. Syst. Ecol.* **1993**, *21*, 57–69. [[CrossRef](#)]
43. Medlin, L.; Elwood, H.J.; Stickel, S.; Sogin, M.L. The characterization of enzymatically amplified eukaryotic 16S-like rRNA-coding regions. *Gene* **1988**, *71*, 491–499. [[CrossRef](#)]
44. Katoh, K.; Standley, D.M. MAFFT multiple sequence alignment software version 7: Improvements in performance and usability. *Mol. Biol. Evol.* **2013**, *30*, 772–780. [[CrossRef](#)]
45. Lindner, A.; Cairns, S.D.; Zibrowius, H. *Leptohelia flexibilis* gen. nov. et sp. nov., a remarkable deep-sea stylasterid (*Cnidaria; Hydrozoa: Stylasteridae*) from the southwest Pacific. *Zootaxa* **2014**, *3900*, 581–591. [[CrossRef](#)]
46. Cairns, S.D.; Lindner, A. A revision of the Stylasteridae (*Cnidaria, Hydrozoa, Filifera*) from Alaska and adjacent waters. *ZooKeys* **2011**, *158*, 1–88. [[CrossRef](#)] [[PubMed](#)]
47. Castresana, J. Selection of conserved blocks from multiple alignments for their use in phylogenetic analysis. *Mol. Biol. Evol.* **2000**, *17*, 540–552. [[CrossRef](#)] [[PubMed](#)]
48. Talavera, G.; Castresana, J. Improvement of phylogenies after removing divergent and ambiguously aligned blocks from protein sequence alignments. *Syst. Biol.* **2007**, *56*, 564–577. [[CrossRef](#)] [[PubMed](#)]
49. Maddison, W.P.; Maddison, D.R. Mesquite: A Modular System for Evolutionary Analysis. Available online: <http://www.mesquiteproject.org> (accessed on 1 October 2021).
50. Lanfear, R.; Calcott, B.; Ho, S.Y.; Guindon, S. PartitionFinder: Combined selection of partitioning schemes and substitution models for phylogenetic analyses. *Mol. Biol. Evol.* **2012**, *29*, 1695–1701. [[CrossRef](#)] [[PubMed](#)]
51. Stamatakis, A. RAxML version 8: A tool for phylogenetic analysis and post-analysis of large phylogenies. *Bioinformatics* **2014**, *30*, 1312–1313. [[CrossRef](#)] [[PubMed](#)]
52. Swofford, D.L. *PAUP: Phylogenetic Analysis Using Parsimony (and Other Methods), Version 4*; Sinauer Associates: Sunderland, MA, USA, 2003.
53. Ronquist, F.; Teslenko, M.; van der Mark, P.; Ayres, D.L.; Darling, A.; Höhna, S.; Huelsenbeck, J.P. MrBayes 3.2: Efficient Bayesian phylogenetic inference and model choice across a large model space. *Syst. Biol.* **2012**, *61*, 539–542. [[CrossRef](#)] [[PubMed](#)]
54. Maggioni, D.; Garese, A.; Huang, D.; Hoeksema, B.W.; Arrigoni, R.; Seveso, D.; Galli, P.; Berumen, M.L.; Montalbetti, E.; Pica, D.; et al. Diversity, host specificity and biogeography in the Cladocorynidae (*Hydrozoa, Capitata*), with description of a new genus. *Cladistics* **2021**, *38*, 13–37. [[CrossRef](#)]
55. Cairns, S.D. A generic revision of the Stylasterina (*Coelenterata: Hydrozoa*). Part 1. Description of the genera. *Bull. Mar. Sci.* **1983**, *33*, 427–508.
56. Broch, H. *Stylasteridae (Hydrocorals)* of the John Murray Expedition to the Indian Ocean. *Sci. Rep. John Murray Exped.* **1947**, *26*, 33–46.
57. Boschma, H. *Stylasterina* in the collection of the Paris Museum: III. *Stylaster flabelliformis* (Lamarck). *Zool. Meded.* **1957**, *35*, 261–282.
58. Schuchert, P. World Hydrozoa Database. Available online: <https://www.marinespecies.org/hydrozoa> (accessed on 20 February 2022).
59. Cairns, S.D.; Samimi-Namin, K. A new species of *Stylaster* (*Cnidaria: Hydrozoa: Stylasteridae*) from the Arabian Sea, off Oman. *Proc. Biol. Soc. Wash.* **2015**, *128*, 209–215. [[CrossRef](#)]

60. Cairns, S.D. Revision of the Hawaiian Stylasteridae (*Cnidaria: Hydrozoa: Athecata*). *Pac. Sci.* **2005**, *59*, 439–451. [[CrossRef](#)]
61. Brooke, S.; Stone, R. Reproduction of deep-water hydrocorals (family *Stylasteridae*) from the Aleutian Islands, Alaska. *Bull. Mar. Sci.* **2007**, *81*, 519–532.
62. Miller, K.J.; Mundy, C.N.; Chadderton, W.L. Ecological and genetic evidence of the vulnerability of shallow-water populations of the stylasterid hydrocoral *Errina novaezelandiae* in New Zealand's fiords. *Aquat. Conserv.* **2004**, *14*, 75–94. [[CrossRef](#)]
63. Purkis, S.J.; Harris, P.M.; Ellis, J. Patterns of sedimentation in the contemporary Red Sea as an analog for ancient carbonates in rift settings. *J. Sediment. Res.* **2012**, *82*, 859–870. [[CrossRef](#)]
64. Giles, E.C.; Saenz-Agudelo, P.; Hussey, N.E.; Ravasi, T.; Berumen, M.L. Exploring seascape genetics and kinship in the reef sponge *Stylissa carteri* in the Red Sea. *Ecol. Evol.* **2015**, *5*, 2487–2502. [[CrossRef](#)]
65. Saenz-Agudelo, P.; Dibattista, J.D.; Piatek, M.J.; Gaither, M.R.; Harrison, H.B.; Nanninga, G.B.; Berumen, M.L. Seascape genetics along environmental gradients in the Arabian Peninsula: Insights from ddRAD sequencing of anemonefishes. *Mol. Ecol.* **2015**, *24*, 6241–6255. [[CrossRef](#)] [[PubMed](#)]
66. Terraneo, T.I.; Fusi, M.; Hume, B.C.; Arrigoni, R.; Voolstra, C.R.; Benzoni, F.; Forsman, Z.H.; Berumen, M.L. Environmental latitudinal gradients and host-specificity shape Symbiodiniaceae distribution in Red Sea *Porites* corals. *J. Biogeogr.* **2019**, *46*, 2323–2335. [[CrossRef](#)]
67. Terraneo, T.I.; Berumen, M.L.; Arrigoni, R.; Waheed, Z.; Bouwmeester, J.; Caragnano, A.; Stefani, F.; Benzoni, F. *Pachyseris inattesa* sp. n. (*Cnidaria, Anthozoa, Scleractinia*): A new reef coral species from the Red Sea and its phylogenetic relationships. *ZooKeys* **2014**, *433*, 1–30. [[CrossRef](#)]
68. Bouwmeester, J.; Benzoni, F.; Baird, A.H.; Berumen, M.L. *Cyphastrea kausti* sp. n. (*Cnidaria, Anthozoa, Scleractinia*), a new species of reef coral from the Red Sea. *ZooKeys* **2015**, *496*, 1–13. [[CrossRef](#)]
69. Terraneo, T.I.; Benzoni, F.; Baird, A.H.; Arrigoni, R.; Berumen, M.L. Morphology and molecules reveal two new species of *Porites* (*Scleractinia, Poritidae*) from the Red Sea and the Gulf of Aden. *Syst. Biodivers.* **2019**, *17*, 491–508. [[CrossRef](#)]
70. Puce, S.; Pica, D.; Schiaparelli, S.; Negrisolo, E. Integration of morphological data into molecular phylogenetic analysis: Toward the identikit of the stylasterid Ancestor. *PLoS ONE* **2016**, *11*, e0161423. [[CrossRef](#)] [[PubMed](#)]